

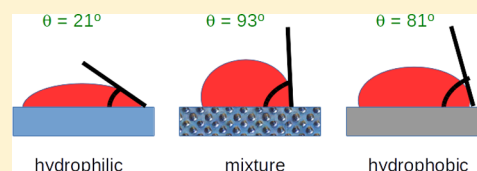
Hydrogen-Bond Heterogeneity Boosts Hydrophobicity of Solid Interfaces

Matías H. Factorovich,[†] Valeria Molinero,[‡] and Damián A. Scherlis^{*,†}

[†]Departamento de Química Inorgánica, Analítica y Química Física/INQUIMAE, Facultad de Ciencias Exactas y Naturales, Universidad de Buenos Aires, Buenos Aires C1428EHA, Argentina

[‡]Department of Chemistry, The University of Utah, 315 South 1400 East, Salt Lake City, Utah 84112-0850, United States

ABSTRACT: Experimental and theoretical studies suggest that the hydrophobicity of chemically heterogeneous surfaces may present important nonlinearities as a function of composition. In this article, this issue is systematically explored using molecular simulations. The hydrophobicity is characterized by computing the contact angle of water on flat interfaces and the desorption pressure of water from cylindrical nanopores. The studied interfaces are binary mixtures of hydrophilic and hydrophobic sites, with and without the ability to form hydrogen bonds with water, intercalated at different scales. Water is described with the mW coarse-grained potential, where hydrogen-bonds are modeled in the absence of explicit hydrogen atoms, via a three-body term that favors tetrahedral coordination. We found that the combination of particles exhibiting the same kind of coordination with water gives rise to a linear dependence of contact angle with respect to composition, in agreement with the Cassie model. However, when only the hydrophilic component can form hydrogen bonds, unprecedented deviations from linearity are observed, increasing the contact angle and the vapor pressure above their values in the purely hydrophobic interface. In particular, the maximum enhancement is seen when a 35% of hydrogen bonding molecules is randomly scattered on a hydrophobic background. This effect is very sensitive to the heterogeneity length-scale, being significantly attenuated when the hydrophilic domains reach a size of 2 nm. The observed behavior may be qualitatively rationalized via a simple modification of the Cassie model, by assuming a different microrugosity for hydrogen bonding and non-hydrogen bonding interfaces.



INTRODUCTION

The behavior of fluids in contact with solid surfaces has been a subject of research for over two centuries, inspiring some of the most renowned scientists of the 19th century, from Young's phenomenological description of the angle formed by a droplet on a homogeneous and flat surface,¹ to the later interpretation of Gibbs who gave a thermodynamic insight into Young's ideas.² Taking Gibbs' work as a starting point, Wenzel and Cassie in the 20th century studied the wetting phenomena of rough and chemically heterogeneous surfaces, respectively, leading to the well-known Wenzel and Cassie–Baxter equations.^{3,4} The former provides the contact angle as a function of rugosity, whereas the latter establishes its dependence on the composition of the interface.

A lot has been done since those early works. Marmur⁵ has described the wetting of a rough surface in two different regimes: one corresponding to the Wenzel equation for slightly rough surfaces, and another for highly irregular morphologies where air can be trapped at the interface, envisioned as a combination of a rough surface with chemical heterogeneity. He also studied the case of droplets on heterogeneous surfaces with periodic patterns, to find that the final contact angle depends on the length of these patterns with respect to the droplet size.⁶ Hysteresis, characterized as the difference between the advancing and receding contact angles, has been experimentally observed in almost all cases.⁷ A few theoretical approaches have been devised for a number of ideal situations,

where the existence of hysteresis was ascribed to roughness and chemical heterogeneity generating local minima in the free energy landscape as a function of the contact angle.^{8–12} This theoretical framework is a key aspect in the rational design of materials for applications related to wetting and spreading.^{13–15} In particular, an understanding of the effect of droplet size on wetting is essential for applications into the nanoscale. Gibbs was the first to formulate a dependence of the contact angle on size,² by introducing the concept of line tension, which is the excess energy associated with the boundary of three bulk phases.^{16–18} As a droplet becomes smaller, the magnitude of the free energy originating in the line tension becomes comparable to the surface tension contribution and influences the final value of the contact angle. This may be of relevance in the nucleation of droplets on surfaces,^{19–21} capillary condensation in pores, or the dynamics of contact line spreading.^{22,23}

Despite the large body of experimental and theoretical research on wettability at the nanoscale, various fundamental questions remain unanswered. The magnitude and even the sign of the line tension are a matter of debate, with reported results spanning 7 orders of magnitude.^{16–18,24–26} Realistic systems combining both chemical heterogeneity and roughness are beyond the scope of the available analytic models, posing a

Received: May 20, 2015

Published: August 4, 2015

challenge to theory and experiments. A nanoscopic understanding of superhydrophobicity and hydrophobic enhancement effects is only starting to emerge.^{27–33} In this context, simulations have played a significant role to elucidate at the nanoscale level the dependence of hydrophobicity on the surface topography, on the molecular interactions and on the droplet size,^{28,30,34,35} and the factors controlling dewetting, nucleation and condensation of water in confinement,^{36,37} or film growth on hydrophobic surfaces.^{38,39} The modeling of heterogeneous surfaces combining polar and nonpolar sites suggests that hydrophobicity is not a linear function of composition, but that important deviations may occur which are dependent on the heterogeneity length-scale,^{28,30,36,40} in line with experimental estimates of interfacial energies.³¹

The purpose of this work is to characterize the hydrophobicity of chemically heterogeneous surfaces as a function of composition and length-scale. Large-scale molecular dynamics simulations are performed to investigate the wettability of a heterogeneous surface resulting from the mixture of hydrophobic and hydrophilic particles, randomly blended at the molecular level, or arranged in patches of different sizes. The hydrophobicity of the interface is assessed in terms of contact angle and desorption pressure. Through the present analysis, we elucidate in what cases the hydrophobicity of an interface turns out to be a linear combination of its chemical components, and what are the factors leading to—sometimes dramatic—deviations from linearity. Finally, we show how the observed behavior can be qualitatively accounted for with a simple modification to the Cassie model.

METHODOLOGICAL APPROACH

Water molecules are described using the mW coarse-grained model, in which each H₂O molecule is treated as a single particle interacting through anisotropic short-ranged potentials that encourage tetrahedrally coordinated structures.⁴¹ In spite of not including electrostatic terms or explicit hydrogen atoms, the mW model is able to accurately reproduce the phase behavior and the thermodynamic properties of water in bulk and in confinement.^{37,39,41–49}

Water is studied on square plates and in cylindrical pores with different hydrophilicities. The particles composing the plates and the pores can have four different kinds of interactions with water: hydrophilic with and without hydrogen bonding, and hydrophobic with and without hydrogen bonding. Thus, we define the four types of particles listed in Table 1, named I, II, III and IV, for which the degree

Table 1. Characterization of the Four Kinds of Particles That May Form the Solid Surface^a

particle	interaction with water	H-bonding	ϵ (kcal/mol)	λ	θ (deg)
I	hydrophilic	no	0.55	0	23
II	hydrophobic	no	0.35	0	82
III	hydrophilic	yes	5.25	23.15	21
IV	hydrophobic	yes	3.50	23.15	81

^aThe parameters ϵ and λ determine the interactions with water (see text). The contact angles (θ) refer to those measured on an amorphous interface made of such particles.

of hydrophilicity and the formation of H-bonds are controlled via the ϵ and λ parameters of the mW model. We note that we classify surfaces II and IV as hydrophobic even if their contact angles fall below 90°, because they resemble the wetting of graphite (86°), which is considered to be hydrophobic. Within the present coarse-grained representation, hydrogen-bonds between water and the solid surface are the result of the three-body term in the Stillinger-Weber potential,

and become manifest in the local tetrahedral order.^{37,39,41,43,45} The ϵ parameter involved in the solid–water interaction was tuned to provide the desired contact angle. Since the three-body term is repulsive, to achieve a given value of θ , a stronger two-body interaction is necessary in the presence of hydrogen bonds ($\lambda = 23.15$) that in their absence ($\lambda = 0$), which explains the different magnitudes of ϵ appearing in Table 1.

Contact angles were measured on square plates of sides ranging from 18 to 55 nm, depending on the size of the droplet. System dimensions are given in Table 2. The thickness of the plates is of 14.5

Table 2. Number of Water Molecules in the Droplet, Size of the Square Plates Employed in the Computation of Contact Angles, and Average Droplet Radii on Different Surfaces: ^atype II; ^btype III; ^catomic scale mixture of types II and III

molecules number	plate size (Å × Å)	droplet radius (Å)
1192	183 × 183	24 ^a /26 ^b /22 ^c
4162	274 × 274	37 ^a /37 ^b
8932	274 × 274	49 ^a /56 ^b /43 ^c
23872	365 × 365	82 ^a /61 ^c
46012	365 × 365	90 ^b /75 ^c
111892	547 × 547	118 ^b /101 ^c

Å, larger than the cut-offs of the water–solid interactions, which are 4.30 and 6.40 Å on the hydrophilic and the hydrophobic surfaces, respectively. Therefore, it is large enough to provide converged results with respect to the normal dimension of the slab. The structures of the plates correspond to amorphous interfaces derived from molecular dynamics simulations of water at 298 K, and composed of the particles defined in Table 1 arranged in three different patterns: randomly, and in hydrophilic spots of 1 and 2 nm diameter. Randomly mixed configurations are generated by replacing, in a random fashion, hydrophilic by hydrophobic particles in a region extending down to 3 Å inside the exposed face. This is done for fractions ranging from 25% to 90%. Plates with circular hydrophilic patches of 10 or 20 Å are made only for a composition of 50%.

The contact angles were measured from the average 3D density profiles of water nanodroplets, following a protocol already established in the literature.^{35,37} Density profiles were sampled on time windows of at least 10 ns after 1 ns of thermalization. Desorption pressures from nanopores were computed using grand canonical molecular dynamics simulations, following the procedure reported elsewhere.³⁷ The diameter of the pores was 28 Å and the length 77 Å, with amorphous walls made of the particles in Table 1 and organized in the same patterns as described for the plates. All simulations were carried out with the LAMMPS code⁵⁰ in periodic boundary conditions. Molecular dynamics were simulated in the canonical ensemble, using the Nosé–Hoover thermostat at 298 K and a time step of 5 fs.

RESULTS AND DISCUSSION

Figure 1 shows the effect of a random intercalation at the atomic level of hydrophilic and hydrophobic particles, on the contact angle of a water droplet of 1192 molecules. The left panel shows that, for a mixture of hydrophilic and hydrophobic particles interacting with water without any orientational preference (particle kinds I and II, $\lambda = 0$), the cosine of the contact angle turns out to be almost linear with respect to composition x_A or x_B . This is the result predicted by the Cassie–Baxter equation,

$$\cos \theta = x_A \cos \theta_A + x_B \cos \theta_B \quad (1)$$

indicated in Figure 1 with a dashed line. Martic and collaborators have already employed molecular simulations to corroborate the validity of the Cassie’s law for a Lennard–Jones

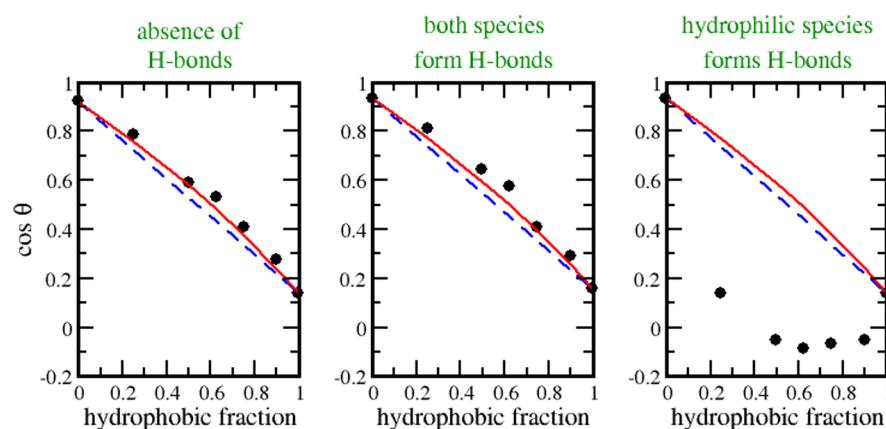


Figure 1. Contact angle as a function of hydrophobic fraction for solid surfaces composed of hydrophilic and hydrophobic molecules randomly mixed at the atomic scale. The circles show the results from simulations, whereas dashed and continuous curves correspond to the Cassie–Baxter and to the Israelachvili–Gee⁵⁴ models, respectively. The labels on top of each panel indicate the composition of the interface. Left: hydrophilic and hydrophobic without H-bonds (I + II). Center: hydrophilic and hydrophobic with H-bonds (III + VI). Right: hydrophilic with H-bonds plus hydrophobic without H-bonds (II + III).

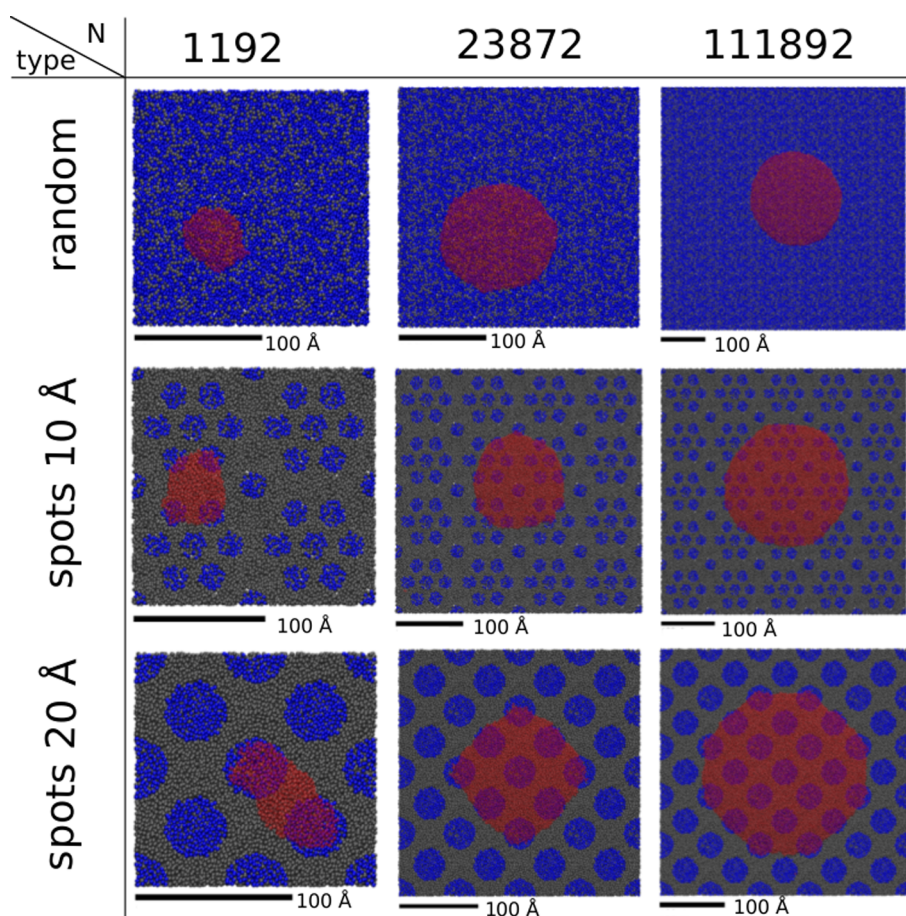


Figure 2. Structures of water droplets (red particles) on plates containing a 50% mixture of hydrophilic (blue) and hydrophobic (gray) molecules in various patterns. From left to right, the number of water molecules N increases. From top to bottom, the heterogeneity length-scale changes from the molecular level to 2 nm spots.

fluid adsorbed on a pore with a randomly heterogeneous surface.⁵¹

If both the hydrophilic and hydrophobic particles can form hydrogen bonds, the situation is similar. The central panel of Figure 1 shows that for a random mixture of particles III and IV, there is also an approximately linear dependence of contact angle with respect to concentration. While it seems unlikely to

observe in nature a hydrophobic interaction involving hydrogen bonds, we have examined this case as a proof of concept.

However, if only one of the species can form hydrogen bonds, we find that the behavior changes dramatically. The right panel of Figure 1 depicts the contact angle as a function of composition for a random mixture of hydrophilic and hydrophobic particles, where only the hydrophilic sites can

form hydrogen-bonds. This combination of particles II and III produces a strong negative deviation from the Cassie–Baxter equation. The synergism is so pronounced, that for a range of compositions, from $x_{\text{II}} \approx 0.4$ to $x_{\text{II}} \approx 0.9$, the hydrophobicity of the mixture becomes larger than that of the purely hydrophobic plate. The largest effect is seen for $x_{\text{II}} \approx 0.65$, when the contact angle exceeds the one corresponding to $x_{\text{II}} = 1$ by 13° . This result is in line with previous observations that a single OH group in a nonpolar background has a stronger effect than the reciprocal combination.^{30,40} The magnitude of this nonlinearity, however, has no precedents in the literature reporting the wettability of chemically heterogeneous interfaces.

The behaviors described above do not seem to be a consequence of the limited size of the droplets. We have performed simulations for increasingly larger droplets, from 1192 to 111892 particles, to assess the impact of the system size on the trend in contact angles. Figure 2 depicts some of the model systems explored, corresponding to water droplets of different sizes on the patterned plates. As the number of molecules in the droplet is increased, thermalization and sampling must be extended over tens of nanoseconds to get a converged result. On the other hand, hysteresis effects become more important and the final contact angle may depend on the starting configuration. These technical issues render these simulations both costly and artful. However, once these issues are overcome, we find that the dependence of the contact angle on the radius of the droplet is very minor. The contact angle as a function of the inverse drop radius is plotted for the different surfaces in Figure 3. The values corresponding to the large

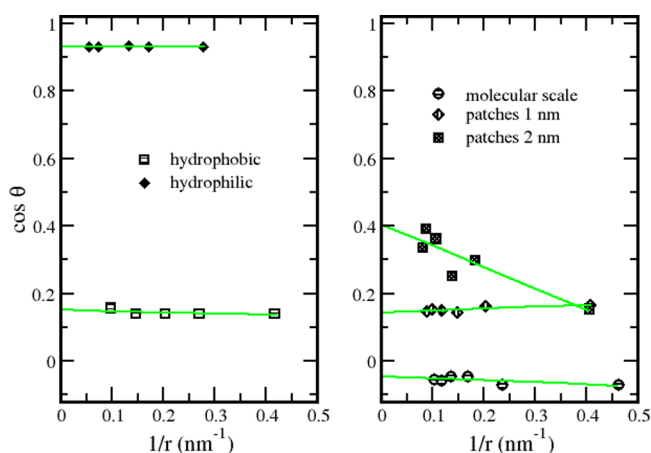


Figure 3. Contact angles as a function of droplet size. Left: pure surfaces of types II and III. Right: 50% mixtures. The straight lines show the linear regressions. The contact angle shows only a minor dependence with respect to radius in the range studied, with the exception of the interface with 2 nm spots, where the dimensions of the heterogeneous pattern is comparable to that of the droplet.

droplets limit (θ_∞), extrapolated from the intercept of the linear regressions, are given in Table 3 for particle types II and

Table 3. Extrapolated Contact Angle for Infinite Radius (θ_∞) as a Function of the Hydrophobic Fraction, for Particle Types II and III^a

X_{pho}	0	0.5	1
θ (deg)	21.5	92.7	81.3

^aFraction of 0.5 corresponds to the atomic scale mixture.

III, and for their atomic scale mixture. The nonadditive behavior is still present if we consider the large droplet limit: the linear combination of θ_∞ of the pure interfaces, equal to 57° , is very far from the value of θ_∞ in the 50% mixture, equal to 93° . These results indicate that the synergism observed in the hydrophilic–hydrophobic mixture does not disappear with the increase in droplet size.

The line tension τ can be estimated from the dependence of contact angle with respect to droplet radius, according to the modified Young equation.⁵² This yields for the hydrophobic, the hydrophilic, and the atomic-scale mixed surfaces, respectively, values of -2.4 ± 6.2 , 0.4 ± 3.5 , and 2.4 ± 5.2 pN. As we have mentioned above, there is no general agreement regarding the magnitude or even the sign of τ , with experimental values for water ranging from 10 to 10^6 pN.⁵³ Large discrepancies have been reported for the same substrates measured with similar approaches that have been ascribed to sample preparation, poor experimental techniques, out of equilibrium measurements, or oversimplifications in the analysis.¹⁶ Comparable discrepancies are also present throughout the theoretical results. One of the most recent experimental studies has settled a value of -30 pN for the line tension of water in hydrophobic cavities,¹⁸ in conflict with the majority of previous reports for solid–liquid–vapor systems, which have yielded a positive sign. Our estimations fall, in magnitude, in the lower range of the existing data. In any case, to the best of our knowledge, the present estimates are the most involved in terms of sampling and system size, if compared with other calculations based on the same approach.

The Cassie–Baxter equation must hold when the size of the hydrophilic and the hydrophobic domains reaches the macroscopic limit. In this context, we have investigated the role of the length of the heterogeneity on the deviation from the linear regime. To this end, we analyzed the water contact angle on plates exhibiting equal fractions of H-bonding hydrophilic and hydrophobic molecules (particles II and III in the same proportions), but arranged in regular hydrophilic patches of 10 and 20 Å diameter. For these systems, the macroscopic contact angles were estimated from linear regressions with respect to the inverse radii, as already done for the random mixtures. The right panel of Figure 3 shows that there is no significant dependence of the contact angle with respect to droplet size on the interface with spots of 1 nm diameter, but this is not the case when this diameter reaches 2 nm and becomes comparable to the dimensions of the droplet. This is evident from the bottom panel of Figure 2, which shows that the droplet of 1192 molecules is strongly distorted by the underlying patterning. The results summarized in Table 4 or Figure 4 indicate that as

Table 4. Extrapolated Contact Angles for Infinite Radius (θ_∞) as a Function of the Length of Heterogeneity for 50% Hydrophobic–Hydrophilic Mixtures of Particles II and III

length (Å)	molecular	10 Å	20 Å	Cassie's law
θ (deg)	92.7	81.8	66.2	57.3

the length of the chemical heterogeneity becomes larger, the nonlinear behavior tends to vanish. In particular, for 2 nm patches the value of θ_∞ falls close to Cassie's law prediction. This makes manifest that the Cassie–Baxter or the Israelachvili–Gee⁵⁴ models do not consider the cooperative effects arising from the molecular heterogeneity of the systems. Such cooperative effects rapidly decrease when the heterogeneity

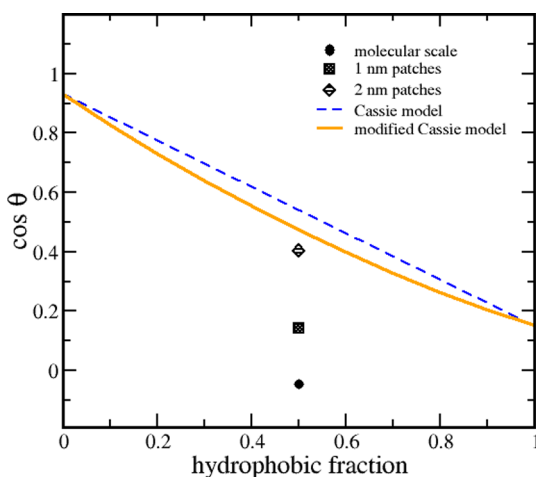


Figure 4. Contact angle as a function of hydrophobic fraction for solid surfaces composed of hydrophilic and hydrophobic molecules of types II and III, intercalated at different length-scales. The orange curve represents the modified Cassie model (eq 4) with a rugosity ratio of 0.6.

length-scale goes above the molecular dimensions, and are clearly attenuated in the case of 20 Å diameter patches.

As an independent measure of hydrophobicity, we computed the desorption pressures of water from cylindrical pores with open ends. Desorption pressures were calculated using the grand canonical screening scheme proposed in our recent work.^{44,55} Vapor desorption from open-ended pores is an equilibrium process which is well described by the Kelvin equation in nanopores down to 3 nm size.^{37,56} The present simulations were performed in 3 nm wide nanopores of 7.7 nm length, displaying the same patterning of hydrophilic and hydrophobic particles already investigated in the plates. The results, depicted in Figure 5, reflect the same trends reported

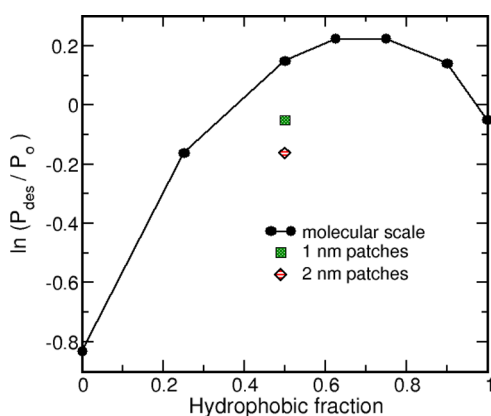


Figure 5. Desorption pressure from a nanopore as a function of the composition of the solid interface. The pore is 3 nm wide and its surface contains hydrophilic and hydrophobic molecules of types II and III intercalated at different length-scales: molecular, and hydrophilic spots of 1 and 2 nm.

for the contact angles: the random mixture of hydrogen-bonding and non hydrogen-bonding surface sites induces a strong deviation from the linear behavior, which appears gradually attenuated when the sizes of the hydrophilic spots are 10 and 20 Å. We calculated contact angles and vapor pressures from two different kinds of computational experiments on

different model systems. The fact that these two independent properties attest a similar hydrophobic enhancement for the same range of compositions is remarkable and reinforces our conclusions of a non-linear effect of hydrogen bond heterogeneity on the contact angle of water.

Our simulations show that a random intercalation at the nanoscale of hydrophilic and hydrophobic molecules is not enough to lead to any significant nonlinear effects: the necessary ingredient to observe the enhancement of the hydrophobicity appears to be the heterogeneity in the formation of hydrogen bonds with water. The question is, then, why does this hydrogen bond heterogeneity boost the hydrophobicity of the interface? Different studies have pointed that a small number of hydrophilic sites on a hydrophobic background may dramatically change the wetting properties of the interface.^{36,57,58} Garde and other authors have explained this effect in terms of the water density fluctuations at the interface.^{29,30,32} From a thermodynamic viewpoint, an answer can be found at the level of the Cassie model, if we think of hydrogen-bond heterogeneity as a rugosity effect. In this way, it is possible to characterize the hydrogen-bonding surface with a different microscopic rugosity than the non-hydrogen-bonding interface. Then, making use of the Wenzel formula, we can rewrite the thermodynamic differential relations leading to eq 1 under the assumption that the hydrophilic and the hydrophobic particles exhibit, respectively, microscopic rugosities r_1 and r_2 . The infinitesimal change in free energy F as a function of contact angle θ for a droplet of radius a on a mixed interface can be written:

$$dF = \gamma_{LV} dS_{LV} + (x_1\gamma_{SL1} + x_2\gamma_{SL2}) dS_{SL} + \gamma_{SV} dS_{SV} \quad (2)$$

$$dS_{LV} = 2\pi a \cos \theta da$$

$$dS_{SL} = -dS_{SV} = f(x_1; x_2)2\pi a da \quad (3)$$

where γ represents interfacial free energies, S is the area, x_1 and x_2 are the molar fractions of species 1 and 2 composing the solid surface, $f(x_1; x_2)$ is its rugosity, and the subindices LV, SL, and SV indicate the liquid–vapor, solid–liquid, and solid–vapor interfaces, respectively. If we assume that the global rugosity is a linear combination of the individual rugosities, $f(x_1; x_2) = x_1r_1 + x_2r_2$, then the equilibrium condition $dF/da = 0$ leads to the following result:

$$\cos \theta = \alpha x_1^2 + \beta x_1 + \delta \quad (4)$$

$$\alpha = \cos \theta_1 + \cos \theta_2 - \frac{r_1}{r_2} \cos \theta_2 - \frac{r_2}{r_1} \cos \theta_1$$

$$\beta = \frac{r_1}{r_2} \cos \theta_2 + \frac{r_2}{r_1} \cos \theta_1 - 2 \cos \theta_2$$

$$\delta = \cos \theta_2$$

where θ_1 and θ_2 are the contact angles on the pure interfaces. The interesting point about this simple model is that it predicts a quadratic behavior for the global contact angle, with negative deviations occurring for $r_1/r_2 < 1$. In particular, Figure 4 shows the prediction of eq 4 if the ratio between the hydrophobic and hydrophilic rugosities is 0.6. For this ratio and $x_1 = 0.5$, the contact angle yielded by the modified Cassie formula falls close to the one obtained in our simulations on 20 Å patches (Table 4). Hence, this rudimentary model seems to be enough to give a qualitative description of the contact angle when the

heterogeneity length-scale is higher than 2 nm. Below this limit, when the heterogeneity reaches the molecular scale, strong deviations are observed which cannot be captured by this approach.

FINAL REMARKS

To conclude, we highlight the most significant findings of this work: (i) on chemically heterogeneous surfaces where the hydrophobic and hydrophilic species present the same kind of coordination with water, contact angles and vapor pressures show a linear behavior with respect to surface composition; (ii) if only the hydrophilic species interacts via hydrogen bonding, pronounced deviations from linearity can be observed, to the extent that the hydrophobicity of the mixture exceeds that of the purely hydrophobic interface; (iii) the strong nonlinear behavior stems from the admixing at the molecular scale, and tends to vanish when the size of the hydrophilic domains goes above 2 nm; (iv) this coordination heterogeneity can be incorporated to the Cassie model by assigning different microscopic rugosities to hydrogen and non-hydrogen bonding surfaces, which explains the nonlinear dependence of the contact angle with respect to composition.

AUTHOR INFORMATION

Corresponding Author

*damian@qi.fcen.uba.ar

Notes

The authors declare no competing financial interest.

ACKNOWLEDGMENTS

This study has been supported by a collaborative grant of the Agencia Nacional de Promocion Cientifica y Tecnologica de Argentina, PICT 2012-2292 to V.M. and D.A.S., and by funding from the University of Buenos Aires, UBACyT 20020120100333BA. We acknowledge the Center of High Performance Computing of The University of Utah for technical support and the allocation of computing time.

REFERENCES

- (1) Young, T. *Philos. Trans. R. Soc. London* **1805**, 95, 65.
- (2) Gibbs, J. W. *The Scientific Papers of J. W. Gibbs*; Dover: New York, 1961; Vol. 1, p 288.
- (3) Wenzel, R. N. *Ind. Eng. Chem.* **1936**, 28, 988.
- (4) Cassie, A. B. D. *Discuss. Faraday Soc.* **1948**, 3, 11–16.
- (5) Marmur, A. *Langmuir* **2003**, 19, 8343–8348.
- (6) Marmur, A.; Bittoun, E. *Langmuir* **2009**, 25, 1277–1281.
- (7) Johnson, R. E.; Dettre, R. H. In *Wettability*; Berg, J. C., Ed.; Marcel Dekker: New York, 1993; pp 1–74.
- (8) Johnson, R. E.; Dettre, R. H.; Brandeth, D. J. *Colloid Interface Sci.* **1977**, 62, 205–212.
- (9) Huh, C.; Mason, S. G. *J. Colloid Interface Sci.* **1977**, 60, 11.
- (10) Joanny, J. F.; de Gennes, P. G. *J. Chem. Phys.* **1984**, 81, 552.
- (11) Extrand, C. W. *Langmuir* **2002**, 18, 7991–7999.
- (12) Long, J.; Hyder, M.; Huang, R.; Chen, P. *Adv. Colloid Interface Sci.* **2005**, 118, 173–190.
- (13) Kijlstra, J.; Reihls, K.; Klamt, A. *Colloids Surf., A* **2002**, 206, 521–529.
- (14) Lu, Y.; Sathasivam, S.; Song, J.; Crick, C. R.; Carmalt, C. J.; Parkin, I. P. *Science* **2015**, 347, 1132–1135.
- (15) Bonn, D.; Eggers, J.; Indekeu, J.; Meunier, J.; Rolley, E. *Rev. Mod. Phys.* **2009**, 81, 739–805.
- (16) Amirfazli, A.; Neumann, A. *Adv. Colloid Interface Sci.* **2004**, 110, 121–141.
- (17) Wang, J. Y.; Betelu, S.; Law, B. M. *Phys. Rev. E: Stat. Phys., Plasmas, Fluids, Relat. Interdiscip. Top.* **2001**, 63, 031601.
- (18) Guillemot, L.; Biben, T.; Galarneau, A.; Vigier, G.; Charlaix, E. *Proc. Natl. Acad. Sci. U. S. A.* **2012**, 109, 19557–19562.
- (19) Law, B. M. *Phys. Rev. Lett.* **1994**, 72, 1698–1701.
- (20) Lazaridis, M. J. *Colloid Interface Sci.* **1993**, 155, 386–391.
- (21) Aleksandrov, A. D.; Toshev, B. V.; Sheludko, A. D. *Langmuir* **1991**, 7, 3211.
- (22) de Gennes, P. G. *Rev. Mod. Phys.* **1985**, 57, 827–863.
- (23) Dussan, E. B. *Annu. Rev. Fluid Mech.* **1979**, 11, 371–400.
- (24) Dobbs, H. *Langmuir* **1999**, 15, 2586–2591.
- (25) Wu, J.; Zhang, M.; Wang, X.; Li, S.; Wen, W. *Langmuir* **2011**, 27, 5705–5708.
- (26) Heim, L.-O.; Bonaccorso, E. *Langmuir* **2013**, 29, 14147–14153.
- (27) Bittoun, E.; Marmur, A. *Langmuir* **2012**, 28, 13933–13942.
- (28) Giovambattista, N.; Debenedetti, P. G.; Rosky, P. J. *Proc. Natl. Acad. Sci. U. S. A.* **2009**, 106, 15181–15185.
- (29) Godawat, R.; Jamadagni, S. N.; Garde, S. *Proc. Natl. Acad. Sci. U. S. A.* **2009**, 106, 15119–15124.
- (30) Acharya, H.; Vembanur, S.; Jamadagni, S. N.; Garde, S. *Faraday Discuss.* **2010**, 146, 353–365.
- (31) Kuna, J. J.; Voitchovsky, K.; Singh, C.; Jiang, H.; Mwenifumbo, S.; Ghorai, P. K.; Glotzer, S. C.; Stellacci, F. *Nat. Mater.* **2009**, 8, 837–842.
- (32) Remsing, R.; Patel, A. J. *Chem. Phys.* **2015**, 142, 024502.
- (33) Rotenberg, B.; Patel, A. J.; Chandler, D. *J. Am. Chem. Soc.* **2011**, 133, 20521–20527.
- (34) Werder, T.; Walther, J. H.; Jaffe, R. L.; Halicioglu, T.; Koumoutsakos, P. *J. Phys. Chem. B* **2003**, 107, 1345–1352.
- (35) Giovambattista, N.; Debenedetti, P. G.; Rosky, P. J. *J. Phys. Chem. B* **2007**, 111, 9581–9587.
- (36) Hua, L.; Zangi, R.; Berne, B. J. *J. Phys. Chem. C* **2009**, 113, 5244–5253.
- (37) Factorovich, M. H.; Gonzalez Solveyra, E.; Molinero, V.; Scherlis, D. A. *J. Phys. Chem. C* **2014**, 118, 16290–16300.
- (38) Hung, S.-W.; Hsiao, P.-Y.; Chen, C.-P.; Chieng, C.-C. *J. Phys. Chem. C* **2015**, 119, 8103–8111.
- (39) Lupi, L.; Kastelowitz, N.; Molinero, V. *J. Chem. Phys.* **2014**, 141, 18C508.
- (40) Giovambattista, N.; Debenedetti, P. G.; Rosky, P. J. *J. Phys. Chem. C* **2007**, 111, 1323–1332.
- (41) Molinero, V.; Moore, E. B. *J. Phys. Chem. B* **2009**, 113, 4008–4016.
- (42) Moore, E. B.; Molinero, V. *Nature* **2011**, 479, 506–508.
- (43) Moore, E. B.; Allen, J. T.; Molinero, V. *J. Phys. Chem. C* **2012**, 116, 7507–7514.
- (44) Factorovich, M. H.; Molinero, V.; Scherlis, D. A. *J. Am. Chem. Soc.* **2014**, 136, 4508–4514.
- (45) de la Llave, E.; Molinero, V.; Scherlis, D. A. *J. Phys. Chem. C* **2012**, 116, 1833–1840.
- (46) Lupi, L.; Hudait, A.; Molinero, V. *J. Am. Chem. Soc.* **2014**, 136, 3156–3164.
- (47) Xu, L.; Molinero, V. *J. Phys. Chem. B* **2010**, 114, 7320–7328.
- (48) Baron, R.; Molinero, V. *J. Chem. Theory Comput.* **2012**, 8, 3696–3704.
- (49) Lu, J.; Qiu, Y.; Baron, R.; Molinero, V. *J. Chem. Theory Comput.* **2014**, 10, 4104–4120.
- (50) Plimpton, S. J. *Comput. Phys.* **1995**, 117, 1–19.
- (51) Martic, G.; Blake, T. D.; Coninck, J. D. *Langmuir* **2005**, 21, 11201–11207.
- (52) Li, D. *Colloids Surf., A* **1996**, 116, 1–23.
- (53) Drelich, J. *Colloids Surf., A* **1996**, 116, 43–54.
- (54) Israelachvili, J. N.; Gee, M. L. *Langmuir* **1989**, 5, 288–289.
- (55) Factorovich, M. H.; Molinero, V.; Scherlis, D. A. *J. Chem. Phys.* **2014**, 140, 064111.
- (56) Fisher, L. R.; Israelachvili, J. N. *Nature* **1979**, 277, 548–549.
- (57) Luzar, A.; Leung, K. *J. Chem. Phys.* **2000**, 113, 5836–5844.
- (58) Willard, A. P.; Chandler, D. *Faraday Discuss.* **2009**, 141, 209–220.